Tetrahedron Vol. 47, No. 47, pp. 9915-9928, 1991
Printed in Great Britain

0040-4020/91 $3.00+.00

CONFORMATIONAL ANALYSIS OF A 7,8-EPOXYCEMBRANOID

Jan-Eric Berg,[a] Aatto Laaksonen[b] and Inger Wahlberg[c]

[a] Department of Structural Chemistry, Arrhenius Laboratory, University of Stockholm, S-10691 Stockholm, Sweden

[b] Department of Physical Chemistry, Arrhenius Laboratory, University of Stockholm, S-10691 Stockholm, Sweden

[c] Reserca AB, S-11884 Stockholm, Sweden

(*Received in UK* 11 *October* 1991)

Abstract: An analysis of the solution conformation of (1*S*,2*E*,4*S*,6*R*,7*R*,8*R*,11*E*)-7,8-epoxy-2,11-cembradiene-4,6-diol (**1**), a tobacco diterpenoid, has been performed by using NMR methods, molecular mechanics calculations and molecular dynamics simulations, and the solid state structure has been determined by X-ray analysis. The results obtained indicate that the solid state structure is essentially retained in solution.

The cembranoids of tobacco form a rapidly growing group of diterpenoids now comprising more than seventy compounds. They are present in a high concentration in the cuticular wax of the leaf and flower of most tobacco varieties, where they co-occur with compounds such as aliphatic hydrocarbons, fatty alcohols and wax esters. The (4*R*)- and (4*S*)-epimers of (1*S*,2*E*,6*R*,7*E*,11*E*)-2,7,11-cembratriene-4,6-diol (**2**, **3**) are the major components and, as suggested by results from biomimetic experiments, the principal precursors of most of the other tobacco cembranoids. The metabolism of the cembranoids also involves breakages of carbon-carbon bonds in the macrocylic ring with the formation of isopropyl-containing carboacyclic products having less than twenty carbon atoms. Some sixty compounds of this type have been encountered in tobacco to-date. Their presence is of considerable interest, since several of these cembrane-derived compounds give significant contributions to the aroma.[1]

It should be noted, however, that the tobacco cembranoids are not only of importance as precursors of aroma compounds. Recent studies have revealed that they have biological functions and also that they exhibit pharmacological

effects. Thus, the two 4,6-diols (**2**, **3**) possess plant growth inhibiting properties,[2] whereas an 11-hydroperoxy-2,6,12(20)-cembratriene-4,8-diol (**4**) has been found to inhibit the activity of indole-3-acetic acid.[3]

Moreover, the levels of cembranoids in the cuticular wax have been associated with insect resistance,[4] and the two 4,6-diols (**2**, **3**) have been reported to inhibit the germination of spores of *Perenospora tabacina* on tobacco.[5] They have also been identified as antitumour promoting agents, a discovery that has aroused considerable interest.[6] The current interest in the tobacco cembranoids is also demonstrated by the fact that total syntheses of the two 4,6-diols (**2**, **3**) have recently been published by Marshall *et al*[7] and by Thomas *et al.*[8]

The determination of the stereostructures of these fourteen-membered ring compounds has hitherto rested heavily on X-ray studies and on chemical correlations with previously known cembranoids. The application of NMR spectroscopy for stereochemical assignments has often been hampered by the scarce information available on their conformation(s) in solution. In fact, only three cembranoids have been subjected to conformational studies to-date, these being denticulatolide (**5**),[9] pachyclavulariolide (**6**)[10] and sarcophytol A (**7**).[11]

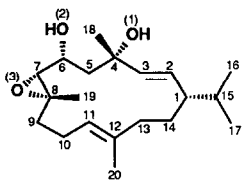

1

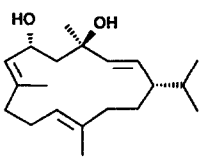

2

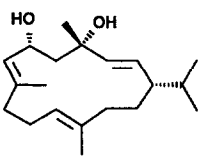

3

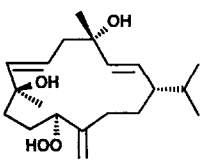

4

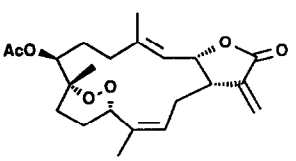

5

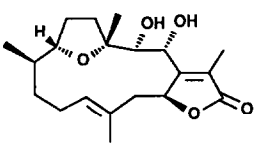

6

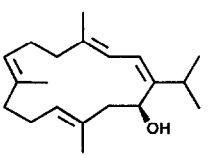

7

This fact and the observation from X-ray analyses that substantial differences exist within the group of tobacco cembranoids with respect to the conformation of the C(4) to C(8) portion of the molecule[12] have encouraged conformational studies. We now report the results obtained for (1*S*,2*E*,4*S*,6*R*,7*R*,8*R*,11*E*)-7,8-epoxy-2,11-cembratriene-4,6-diol (**1**), a tobacco constituent,[13] by using X-ray diffraction analysis, NMR methods, molecular mechanics (MM2) calculations and molecular dynamics (MD) simulations.

RESULTS AND DISCUSSION

Crystallography.

Bond lengths and bond angles, both with estimated standard deviations, are listed in Table 1. Crystal and experimental data are given in Table 6. Fig. 1 is a stereoscopic drawing of the molecule.

The maximum, minimum and mean values of the sp^3-sp^3 bonds are 1.561 (12), 1.453 (12), and 1.518 Å; the corresponding values of the sp^2-sp^2 bonds are 1.353 (12), 1.313 (10) and 1.333 Å. All bond angles are within the expected range. The hydroxy groups at C(4) and C(6) are intramolecularly hydrogen-bonded to each other, the distance between acceptor and donor being 2.726 Å. One short intermolecular hydrogen bond O(3) - O(2a) where (a) is related by the symmetry operation -1.0-y, x, -0.25+z, has a distance of 2.822 Å. The shortest intramolecular non-bonded distance of 2.405 Å is between C(7) and O(2).

Table 1.

Bond lengths (Å) in epoxide **1.**

C(4)-O(1)	1.438(8)	C(6)-O(2)	1.431(9)
C(7)-O(3)	1.442(8)	C(8)-O(3)	1.469(9)
C(2)-C(1)	1.560(11)	C(3)-C(2)	1.313(10)
C(4)-C(3)	1.490(10)	C(5)-C(4)	1.537(12)
C(18)-C(4)	1.511(11)	C(6)-C(5)	1.542(12)
C(7)-C(6)	1.499(10)	C(8)-C(7)	1.453(12)
C(9)-C(8)	1.493(12)	C(19)-C(8)	1.516(11)
C(10)-C(9)	1.561(13)	C(11)-C(10)	1.479(12)
C(12)-C(11)	1.353(12)	C(13)-C(12)	1.495(13)
C(20)-C(12)	1.509(14)	C(14)-C(13)	1.530(12)
C(16)-C(15)	1.516(14)	C(17)-C(15)	1.517(12)

Bond angles (deg.) in epoxide **1.**

C(8)-O(3)-C(7)	59.9(5)	C(14)-C(1)-C(2)	112.3(6)
C(15)-C(1)-C(2)	110.0(6)	C(15)-C(1)-C(14)	111.6(6)
C(3)-C(2)-C(1)	125.7(7)	C(4)-C(3)-C(2)	127.7(7)
C(3)-C(4)-O(1)	111.3(7)	C(18)-C(4)-C(5)	108.7(7)
C(5)-C(4)-O(1)	109.3(6)	C(5)-C(4)-C(3)	112.6(7)
C(18)-C(4)-O(1)	106.7(7)	C(18)-C(4)-C(3)	108.0(6)
C(6)-C(5)-C(4)	118.2(7)	C(5)-C(6)-O(2)	108.0(7)
C(7)-C(6)-O(2)	110.2(7)	C(7)-C(6)-C(5)	112.8(6)
C(6)-C(7)-O(3)	116.2(7)	C(7)-C(8)-O(3)	59.1(5)
C(8)-C(7)-O(3)	61.0(5)	C(8)-C(7)-C(6)	124.7(7)
C(9)-C(8)-O(3)	113.5(6)	C(9)-C(8)-C(7)	120.0(7)
C(19)-C(8)-O(3)	114.0(7)	C(19)-C(8)-C(7)	121.0(7)

Table 2. Observed and Calculated Vicinal Coupling Constants (in Hz) in the Solid State Structure, the Minimized Solid State Structures and Conformers A-G.

H-H	Observed		Calculated										
	$CDCl_3$	CD_3OD	X-Ray	X-Ray ε=1.5	A	B ε=1.5	C	X-Ray	D ε=4.8	E	X-Ray	F ε=33.6	G
5a-6	1.0	1.0	0.9	1.1	0.9	1.1	1.6	1.0	1.0	1.0	0.9	0.9	0.9
5b-6	6.8	7.0	6.5	8.6	7.4	8.7	5.2	8.3	8.3	8.3	8.2	8.2	8.2
6-7	9.2	9.0	9.3	8.3	7.0	7.8	7.3	8.2	7.9	7.8	8.2	7.9	7.8
9a-10a	12.8	13.0	13.6	13.4	13.6	13.3	13.5	13.5	13.5	13.5	13.5	13.5	13.6
9a-10b	3.9	3.6	2.3	3.5	2.5	3.9	1.5	3.3	3.3	2.8	3.2	3.2	2.7
9b-10a	3.7	3.5	2.7	3.7	2.7	4.0	1.6	3.4	3.4	2.9	3.3	3.3	2.8
9b-10b	4.3	5.0	3.4	3.1	4.3	2.9	5.7	3.4	3.4	4.0	3.5	3.5	4.1
13a-14a	4.2		2.6	3.1	3.1	3.1	3.0	3.1	3.1	4.1	3.1	3.1	4.0
13a-14b	4.3		3.7	3.9	3.9	3.9	4.1	3.9	3.9	3.1	3.9	3.9	3.1
13b-14a	3.8		2.6	3.8	3.9	3.8	4.0	3.8	3.8	3.0	3.8	3.8	3.1
13b-14b	12.9		13.0	13.0	13.0	13.0	12.9	13.0	13.0	13.2	13.0	13.0	13.2
14a-1	12.1		12.4	12.3	12.3	12.3	12.4	12.3	12.3	11.7	12.3	12.3	11.7
14b-1	3.2		3.3	2.1	2.3	2.1	2.6	2.2	2.1	4.7	2.2	2.1	4.7

Table 1. continued

C(19)-C(8)-C(9)	115.4(8)	C(10)-C(9)-C(8)	112.3(7)
C(11)-C(10)-C(9)	112.4(7)	C(12)-C(11)-C(10)	128.8(8)
C(13)-C(12)-C(11)	120.4(9)	C(20)-C(12)-C(11)	122.0(9)
C(20)-C(12)-C(13)	117.6(9)	C(14)-C(13)-C(12)	116.9(7)
C(13)-C(14)-C(1)	116.1(7)	C(16)-C(15)-C(1)	114.5(6)
C(17)-C(15)-C(1)	112.2(7)	C(17)-C(15)-C(16)	111.4(7)

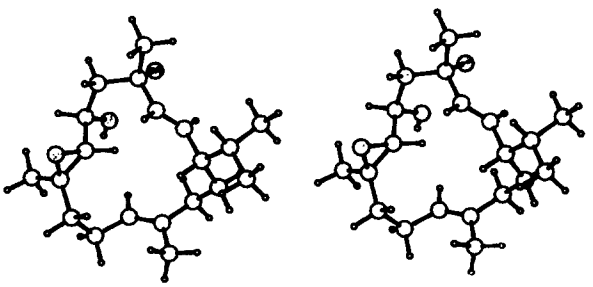

Fig. 1. A stereoscopic view of (1*S*,2*E*,4*S*,6*R*,7*R*,8*R*,11*E*)-7,8-epoxy-2,11-cembradiene-4,6-diol (**1**).

NMR Methods.

Having determined the conformation of **1** in the solid state, NMR methods were used to explore whether this conformation is significantly populated in solution. To this end, the vicinal coupling constants, $^{3}J_{H,H}$, for the X-ray structure were calculated by using a generalized Karplus equation. [14, 15] As shown in Table 2, the values obtained agree well enough with those measured experimentally to suggest that the solid state conformer is essentially retained in solution. It is also evident from Table 2 that the coupling constants measured in $CDCl_3$ are close to those measured in CD_3OD, which would indicate a high conformational homogeneity. This view is consistent with the relative large chemical shift differences[10] between the diastereotopic protons at C(5), C(9), C(10) and C(14), respectively, those at C(13) being a possible exception (Table 3).

Table 3. Diastereotopic ^{1}H Chemical shifts (δ) and Differences (Δδ) in ppm.

Solvent	H-5a/H-5b	H-9a/H-9b	H-10a/H-10b	H-13a/H-13b	H-14a/H-14b
$CDCl_3$	1.97/2.25 (0.28)	1.05/2.10 (1.05)	1.91/2.34 (0.43)	2.14/2.16 (0.02)	1.44/1.7 (0.27)
CD_3OD	1.86/2.14 (0.28)	1.03/2.05 (1.02)	1.91/2.32 (0.41)	a	a

a) Not visible

Molecular Mechanics Calculations.

In order to obtain support for the view that the conformation in the solid state is highly populated in solution, molecular mechanics calculations, MM2(87),[16] were performed. In view of the obvious difficulties in making a thorough selection of input geometries of this macrocyclic compound from Dreiding models, a dihedral angle driver computer program, RNGCFM,[17] which generates conformers in a systematic manner, was used. By using an angle increment of 20°, some 1300 initial geometries were obtained. Some 900 of these were subjected to energy minimization. To simulate the influence of solvation the calculations were carried out using three different dielectric constants in the force field.

The resultant conformers, obtained when an ε-value of 1.5 (gas phase) was used, had relative steric energies ranging from 0 to 23 kcal/mole. Those falling into the energy range 0 - 2.3 kcal/mole, in all 11, were selected for further study. They converged into three groups, **A** - **C**, with respect to energy level and to geometry, polar maps thereby being useful tools. Conformers **D** - **E** (energy range 0 - 1.9 kcal/mol) and **F** - **G** (energy range 0 - 2.0 kcal/mol) were the conformers of lowest energy that were obtained when an ε-value of 4.8 ($CDCl_3$) and 33.6 (CD_3OD), respectively, were used in the minimization (Fig. 2). Groups **A** - **C**, **D** - **E** and **F** - **G** represent 97.6%, 98.8% and 99.3%, respectively, of the Boltzman population of the conformation space.

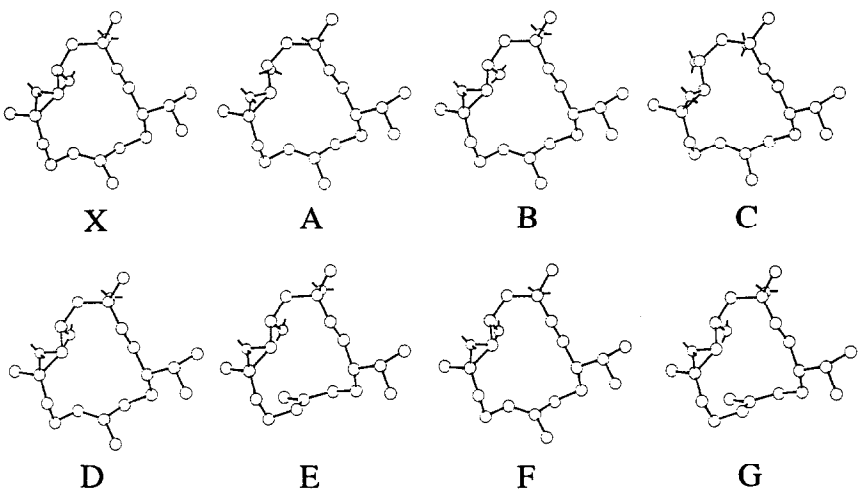

Fig. 2. Plots of the energy-minimized solid state structure (**X**) and conformers **A** - **G**.

Table 4. Endocyclic Torsion Angles (deg.) in **1** Observed by X-Ray Diffractometry and Calculated by Molecular Mechanics (ε=1.5, 4.8 and 33.6) and Molecular Dynamics.

Torsion Angle	Observed	Calculated											
	X-ray Structure	Minimized X-Ray ε=1.5	A	B	C	Minimized X-Ray ε=4.8	D	E	Minimized X-Ray ε=33.6	F	G	Molecular Dynamics $CHCl_3$	Molecular Dynamics CH_3OH
1-2-3-4	179.3	179.7	-178.4	178.0	-175.6	179.8	179.7	-173.8	179.9	-179.8	-173.6	- 179.1(1.3)	178.9(1.5)
2-3-4-5	124.6	114.0	131.2	116.6	138.9	116.7	117.9	117.9	117.5	118.3	118.5	101.1(3.3)	106.8(8)
3-4-5-6	-55.3	-50.3	-63.8	-50.5	-66.4	-53.4	-53.7	-51.7	-54.4	-54.7	-53.0	-56.5(1.0)	-50.0(1.2)
4-5-6-7	78.3	88.3	80.3	89.5	65.8	86.0	86.0	86.7	85.5	85.3	86.0	101.2(2.8)	86.6(3.7)
5-6-7-8	147.7	152.2	166.6	159.8	165.0	153.4	158.6	159.2	153.7	158.2	159.5	149.1(7)	161.2(4.0)
6-7-8-9	155.6	155.3	160.3	155.6	161.4	157.4	157.0	159.3	157.9	157.6	160.4	154.9(2.5)	152.7(5.0)
7-8-9-10	-82.4	-95.6	-96.9	-99.4	-85.9	-95.2	-98.1	-95.3	-95.1	-97.6	-95.5	-90.4(7)	-95.0(2.9)
8-9-10-11	61.3	55.7	62.6	53.3	71.3	57.4	57.2	66.8	58.0	58.0	67.4	54.8(8)	58.7(2.0)
9-10-11-12	94.2	104.7	103.3	113.5	90.8	103.3	108.0	-112.4	102.8	106.9	-112.0	92.8(1.1)	104.6(3.6)
10-11-12-13	179.1	177.2	176.2	177.1	175.7	177.6	177.9	-177.5	177.6	178.1	-177.7	178.1(2.6)	177.0(8)
11-12-13-14	135.1	131.8	126.6	127.6	127.3	131.2	126.9	-7.0	131.0	126.8	-8.0	141.4(1.1)	125.1(4.8)
12-13-14-1	-62.3	-58.4	-58.4	-58.4	-57.9	-58.6	-58.2	-65.0	-58.6	-58.2	-64.5	-60.5(5)	-58.2(6)
13-14-1-2	56.0	62.5	60.6	63.2	57.4	61.9	63.1	41.0	61.6	63.1	41.2	50.0(8)	58.1(1.0)
14-1-2-3	151.6	161.1	160.9	161.5	157.9	161.4	163.9	153.1	161.5	164.3	153.8	154.7(3.3)	160.5(2.8)
Rel. Steric Energy (kcal)			0	1.22	2.27		0	1.89		0	2.02		

The endocyclic torsion angles in the X-ray structure, the energy-minimized X-ray structures and conformers **A** - **G** are listed in Table 4. Of conformers **A** - **C** (ε=1.5), a good correspondence with the solid state structure, particularly that obtained after minimization, is observed for conformers **A** and **B**. The main differences among conformers **A** - **C** reside in the geometry of the C(4) to C(8) portion. It is also noteworthy that the hydroxy groups at C(4) and C(6) are hydrogen-bonded to each other in all three conformers. In conformer **A** hydrogen bonding is also found between the hydroxy hydrogen at C(6) and the epoxide oxygen.

Conformers **D** and **F**, the species of lowest energy obtained with ε=4.8 and 33.6, respectively, are virtually identical with conformer **B** and consequently also with the solid state structure. Conformers **E** and **G** are also essentially identical. They differ from conformers **D** and **F** primarily with respect to the C(10) to C(14) portion of the molecule.

The vicinal coupling constants were next calculated for the energy-minimized solid state structures (ε=1.5, 4.8 and 33.6) and conformers **A** - **G**. It can be seen from the results presented in Table 2 that the values calculated for conformers **A**, **B**, **D** and **F** agree well with those calculated for the solid state structures and those observed in solution. It is noteworthy that the best agreement between the coupling constants measured and those calculated is found for the solid state structure (not energy-minimized). The reason for this may probably be attributed to the fact that the parameters used in the minimizations, particularly those for the epoxide group, are not accurate enough.

Molecular Dynamics Simulations.

Since there is always a potential hazard of being trapped in local minima in the conformation space when performing molecular mechanics types of calculations, molecular dynamics simulations (MD) were used to verify the results. Another purpose of the MD study was to evaluate the molecular solvent effects on the conformation of **1** and to examine the solvent structure around the molecule.

The simulations were performed on **1** in methanol and chloroform, the corresponding deuterated solvents being used in the parallel NMR study. In both simulations, two molecules of **1** were dissolved in 254 solvent molecules in a cubic cell. Experimental densities were chosen and both simulations were carried out at 275 K. Compound **1** was kept fully flexible during the simulation, while the solvent molecules were treated as rigid.

The results indicate that the three-dimensional structure of **1** is very stable and resistant against collisions with solvent molecules. The conformation produced shows no major deviation as compared with that in the solid state (Table 5). The largest fluctuations (rms) are found in methanol solution for the torsion angles involving the hydroxy oxygen atoms attached to C(4) and C(6) [O(1) and O(2)]. These groups are exposed to the solvent molecules due to their polarity and involvement in hydrogen bonds with the methanolic hydroxy groups (see below).

Some insight into the intermolecular interactions was obtained by studying the configurational potential energies in the system. These energies are listed in Table 5; the coulombic and non-coulombic contributions are separated. It can be concluded that the two molecules of **1** interact very weakly with each other in the solution. The coulombic and non-coulombic contributions nearly cancel in both solutions. The fact that the solvents used differ very much from each other can be seen both in the interactions of **1** with the solvent and in the solvent-solvent interactions. The coulombic energy is predominant for methanol, while the interactions involved in the case of chloroform are mainly of short range and of non-coulombic origin.

Table 5. Contributions to the intermolecular potential energy in the MD simulations of epoxide **1** in methanol and chloroform, respectively. Coulombic and non-coulombic energies are separated. All energies are in kcal/mole.

		In Methanol	In Chloroform
Epoxide **1** -Epoxide **1**	Coulombic	-104.0 ± 4.0	-125.7 ± 2.5
	Non-coulombic	101.9 ± 2.1	83.4 ± 3.0
Epoxide **1**-solvent	Coulombic	-91.7 ± 5.2	-39.5 ± 3.4
	Non-coulombic	-71.2 ± 4.3	-114.1 ± 4.5
Solvent-solvent	Coulombic	-1863 ± 102	-91.4 ± 9.2
	Non-coulombic	-295 ± 19	-1643 ± 26

The solvation structure analysis has been limited to the vicinity of the polar groups in **1**, i. e. the hydroxy oxygen atoms at C(4) and C(6) and the epoxy oxygen atom [O(1), O(2) and O(3)]. Calculation of radial distribution functions (RDF), which is a convenient method to examine the solvent structure, was applied. Fig. 3a shows the RDF between O(1) and the hydroxy hydrogen (solid line) and oxygen (dashed line) in methanol. A very sharp and intense peak is present at a distance of 1.8 Å from the O(1) oxygen. This peak is due to a stable hydrogen bond between the two hydroxy groups. Integration shows that one single molecule of methanol is responsible for this peak. Further integration behind the second maximum up to 4.8 Å gives four additional molecules of methanol in the neighbourhood. In the corresponding RDF curve between O(2) and the hydroxy hydrogen (solid line) and oxygen (dashed line) in methanol the first minimum appears at a distance of 3 Å, which is behind the range of a possible hydrogen bond (Fig. 3b). By contrast, the RDF curve between O(3) and the hydroxy hydrogen (solid line) and oxygen (dashed line) in methanol contains a characteristic hydrogen bond peak (Fig. 3c). Integration is consistent with 1.4 molecules of methanol being involved in hydrogen bonding, which means that occasionally two molecules

of methanol are hydrogen bonded to O(3) at the same time.

The RDF curves between the central carbon atom in chloroform and O(1) (solid line), O(2) (dashed line) and O(3) (dash-dotted line) in **1** all have similar shapes with the first maximum at 3.4-3.5 Å indicating that there are no hydrogen bonds (Fig. 3d).

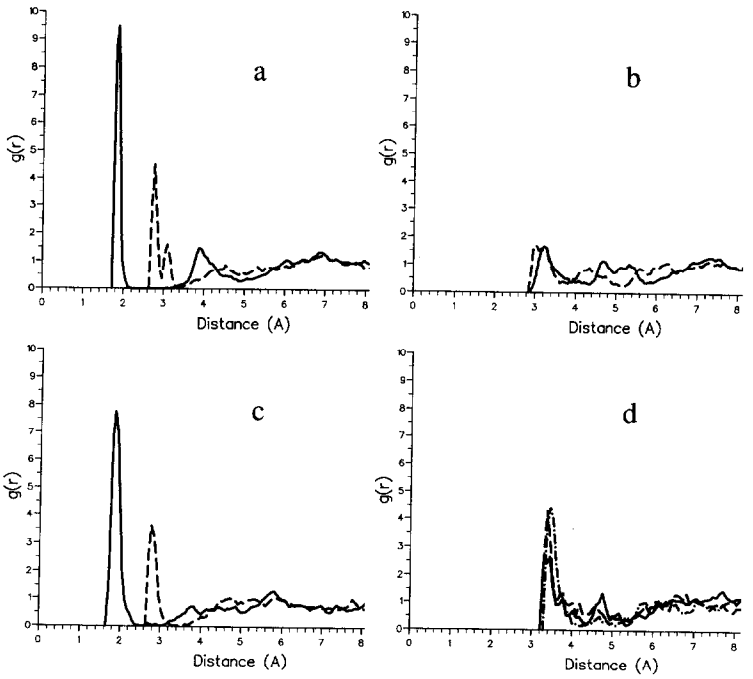

Fig. 3. Radial distribution functions between O(1), O(2) and O(3) in**1** and methanol (**a-c**) and chloroform (**d**).

a) ___ O(1) - MeO(**H**), ---O(1) - Me(**O**)H b) ___ O(2) - MeO(**H**), ---O(2) - Me(**O**)H

c) ___ O(3) - MeO(**H**), ---O(3) - Me(**O**)H d) ___ O(1) - (**C**)HCl_3, ---O(2) - (**C**)HCl_3

_.-.-_ O(3) - (**C**)HCl_3

Molecular dynamics techniques are normally used to access dynamical information about translational, rotational and reorientational motion. These data can then be compared to experimental results such as correlation times from spectroscopic measurements. In the present case we have only measured the translational diffusion coefficients Dv from the molecular centre of mass mean square displacements.

For methanol and chloroform the diffusion coefficient is obtained as 1.2 and 2.1 ($x10^{-9}$ m^2/s), respectively, at 275 K. The corresponding results from the simulations of the pure liquids are 1.7 (at 299 K)[19] and 2.6 (at 295 K)[20] using the same interactions potentials.

Compound **1** shows a very slow diffusional mobility in solution: in methanol 0.9×10^{-12} m^2/s and in chloroform 0.8×10^{-11} m^2/s. Since there is not a large deviation in the viscosity values between the two solvents, the fact that the diffusional motion is one order of magnitude slower in methanol may be accounted for by the stronger interactions between **1** and this solvent.

In spite of the different set of interaction potentials used, explicit inclusion of two different solvents and long simulation runs (50 ps), the conformational results obtained are remarkably consistent with those from the X-Ray, NMR and molecular mechanics studies.

EXPERIMENTAL PART

X-Ray Crystallography Study.

Single crystals of **1** were obtained by recrystallization from a mixture of hexane and ethyl acetate. The space group symmetry was determined from systematic absences and by the unit cell parameters found by the least-squares method from 18 centered reflections. The intensity stability was checked by measurement of three standard reflections ($22\bar{4}$, $13\bar{1}$, $33\bar{1}$) every 60 minutes. The intensities were corrected for Lorentz and polarization corrections but no correction was made for absorption.

In all, 20 of the 22 non-hydrogen atoms were found by direct methods using MULTAN80, while the remaining two non-hydrogen atoms were located from electron-density difference maps. Except for the hydroxy hydrogens, which were not found, all hydrogen atoms were geometrical placed and refined. Full matrix least-squares anisotropic refinement of the non-hydrogen parameters was applied using the SHELX76 program. The hydrogen parameters were refined with all isotropically temperature factors constrained to a common value and bond lengths restricted to 1.00 Å. The strongest reflection (004) was omitted due to extinction effects. The atomic scattering factors used for the non-hydrogen and hydrogen atoms were those included in SHELX76 program (Table 6). Lists of refined coordinates have been deposited at the Cambridge Crystallographic Data Centre.

Table 6. Crystal and Experimental data for (1*S*,2*E*,4*S*,6*R*,7*R*,11*E*)-7,8-Epoxy-2,11-cembradiene-4,6-diol (**1**).

Formula	$C_{20}H_{34}O_3$
Formula weight	306.49
Space group	$P4_3$
Unit cell dimensions	a=9.7665(9), b=9.7665(9) c=20.5908(24) Å
Unit cell volume, V	1964.04(34) $Å^3$

Table 6 continued.

Formula units per unit cell, Z	4
Calculated density, D_x	1.04 g.cm^{-3}
Radiation	Mo Kα
Wavelength, λ	0.71069 Å
Linear absorption coefficient	0.60 cm^{-1}
Temperature, T	293(1) K
Crystal shape	Prismatic
Crystal size	0.10x0.04x0.34 mm
Diffractometer	Siemens/Stoe AED 2
Determination of unit cell:	
Number of reflections used	18
θ-range	12.5 to 25.0°
Intensity data collection:	
Maximum $\sin(\theta)/\lambda$	0.65 Å^{-1}
Range of h, k and l	0 to 8, 0 to 8 and 0 to 17
Standard reflections	3
Intensity instability	< 6 %
Internal R value	0.031
Number of unique reflections	1046
Number of observed reflections	2022
Criterion for significance	$F > 2.5\sigma(F)$
Structure refinement:	
Minimization of	$\Sigma w\Delta F^2$
Anisotropic thermal parameters	All non-hydrogen atoms
Isotropic " "	hydrogen atoms
Number of refined parameters	223
Weighting scheme	$(\sigma^2(F)+0.0020\|F\|^2)^{-1}$
Final R for observed refls.	0.067
" wR " " "	0.073
" wR " all 2022 "	0.123
" $(\Delta/\sigma)_{max}$	0.24
" $\Delta\rho_{min}$ and $\Delta\rho_{max}$	-0.21 and 0.23 e/Å^3

NMR Spectroscopy.

A Varian XL-300 instrument operating at 300 MHz for proton and at 75 MHz for carbon was used to record the 1D and 2D NMR spectra at ambient temperature. After identification of the signals in the ^{1}H NMR spectrum with the aid of ^{1}H-^{1}H and ^{1}H-^{13}C shift correlation spectroscopy, the ^{1}H-^{1}H coupling constants were determined by means of spin simulation techniques. $CDCl_3$ and CD_3OD were used as solvents for these NMR spectra.

Computational Methods.

The possible conformers of **1** used in the MM calculations were generated by using the computer program RNGCFM (QCPE No. 510).[14] The following parameters were used: angle increment 20°, ring closure bond length

limits 1.3-1.7 Å, bond closure angle limits 106-130 °, dihedral closure tolerance limits 25 °, vdW radii scale 0.8, no ring constraints. The structures obtained were subjected to energy minimization employing the computer program MM2 (87).[16]

The vicinal coupling constants, $^3J_{H,H}$, were calculated by using an empirically generalized Karplus equation developed by Haasnoot, de Leeuw and Altona[15] and applied in the program 3JHHPC (QCPE No. QCMPO25).[14]

The Amber force field[18] was used for **1** together with the crystallographic equilibrium distances and bond and torsion angles in the MD simulations. The H1 model of Haughney and coworkers[19] was chosen for methanol, while the potential model of Dietz and Heinzinger[20] was used for chloroform. Simple combination rules were employed for the cross interactions. A modified version of the McMOLDYN package[21] was used to perform the MD simulations. These were done on a Convex C220 computer, the total time covered being 50 pico seconds in both simulations.

The MD simulations were started with an equilibration period of 20-30 pico seconds. During the equilibration the temperature was raised several hundred Kelvin in order to produce transitions over intramolecular energy barriers. The final simulations were carried out at 275 K and during 50 pico seconds.

Acknowledgements.

We are grateful to Professors Peder Kierkegaard and Curt Enzell and to Dr. Arne Björnberg for their support of this work.

REFERENCES

1. Wahlberg, I.; Enzell, C. R. *Nat. Prod. Rep.* **1987**, *4*, 237.
2. Cutler, H. G.; Reid, W. W; Deletang, J. *Plant Cell Physiol.* **1977**, *18*, 711.
3. Koseki, K.; Saito, F.; Kawashima, N.; Noma, M. *Agr. Biol. Chem.* **1986**, *50*, 1917.
4. Johnson, A. W.; Severson, R. F. *J. Agr. Entomol.* **1984**, *1*, 23.
5. Lawson, D. R.; Danehower, D. A.; Shilling, D. G.; Menetrez, M. L.; Spurr, H. W. *Am. Chem. Soc. Symp.* **1988**, *380*, 363.
6. Saito, Y.; Takizawa, H.; Konishi, S.; Yoshida, D.; Mizusaki, S. *Carcinogenesis* **1985**, *6*, 1189.
7. Marshall, J. A.; Robinson, E. D.; Lebreton, J. *J. Org. Chem.* **1990**, *55*, 227.
8. Astles, P. C.; Thomas, E.J. *Synlett* **1989**, 42.
9. Fukazawa, Y.; Usui, S.; Uchio, Y.; Shiobara, Y.; Kodama, M. *Tetrahedron Letters* **1986**, *27*, 1825.

10. Inman, W.; Crews, P. *J. Org. Chem.* **1989**, *54*, 2526.
11. Kobayashi, M.; Kobayashi, K.; Nomura, M.; Munakata, H. *Chem. Pharm. Bull.* **1990**, *38*, 815.
12. Wahlberg, I.; Arndt, R.; Wallin, I.; Vogt, C.; Nishida, T.; Enzell, C. R. *Acta Chem. Scand.* **1984**, *B38*, 21.
13. Wahlberg, I.; Eklund, A.-M.; Vogt, C.; Enzell, C. R.; Berg, J.-E. *Acta Chem. Scand.* **1986**, *B40*, 855.
14. Petillo, P. A., Department of Chemistry, University of New Hampshire, Durham, New Hampshire 03824, USA after Jaime, C. and Osawa, E., Department of Chemistry, Faculty of Science, Hokkaido University, Sapporo 060, Japan. QCPE No. QCMPO25.
15. Haasnoot, C. A. G.; de Leeuw, F. A. A. M.; Altona, C. *Tetrahedron* **1980**, *36*, 2783.
16. Allinger, N. L. Department of Chemistry, The University of Georgia, Athens, Georgia, USA.
17. Smith, G. M., Merck Sharp & Dohme Research Laboratories, Rahway, New Jersey 07065, USA. QCPE No. 510.
18. Weiner, S. J.; Kollman, P. A.; Case, D. A.; Singh, U. C.; Ghio, C.; Alagona, G.; Profeta Jr, S.; Weiner, P. *J. Am. Chem. Soc.* **1984**, *106*, 765.
19. Haughney, M.; Ferrario, M.; McDonald, I. R. *Mol. Phys.* **1986**, *58*, 849.
20. Dietz, W.; Heinzinger, K. *Ber. Bunsenges. Phys. Chem.* **1985**, *89*, 968.
21. Laaksonen, A. *Comp. Phys. Comm.* **1986**, *42*, 271.